Tectonic setting of outer trench slope volcanism: pillow basalt and limestone in the Taconian orogen of eastern New York

Ed Landing, Georgia Pe-Piper, William S.F. Kidd, and Karem Azmy

Abstract: The only pillow basalt in synorogenic sedimentary rocks at the exterior margin of the Taconic orogen in eastern North America is at Stark's Knob in eastern New York. Earlier reported as extrusive into allochthonous Ordovician slope and rise facies, this small lens (ca. 125+ m long, 39 m thick) is a fault-bounded block in Upper Ordovician melange under the Taconian frontal thrust. Its N-MORB (normal mid-ocean ridge basalt) basalt geochemistry and spinel composition are characteristic of oceanic ridge settings at a water depth of 2 km or more. Abundant limestone lenses on pillows and lava shelves within pillows yielded a middle Late Ordovician gastropod. The limestones are reconciled with this extrusion depth and with limited early Paleozoic pelagic carbonate production by lime mud transport from the Laurentian platform or abiotic carbonate precipitation with sea-water heating during basalt extrusion. A genetic relationship between the parautochthonous Stark's Knob basalts and the allochthonous Jonestown volcanics in slope and rise facies of the Hamburg klippe, eastern Pennsylvania, is likely. Both are Ordovician MORB basalts that reflect volcanism on the subducting outer trench slope prior to the Taconic arc – Laurentia collision. Taconic orogenesis may have led to basalt production on the subducting plate by (1) the setting up of orogen-parallel, predominantly strike-slip motion on the subducting slab with MORB basalt generated at offsets in a setting analogous to the Gulf of California or (2) development of faults in a flexure-induced extensional regime. By either process, mafic volcanism appears to be a rare but tectonically significant process on outer trench slopes as continental margins or oceanic plates enter subduction zones.

Résumé : L'unique basalte à coussinet dans les roches sédimentaires syntectoniques à la bordure extérieure de l'orogène taconique dans l'est de l'Amérique du Nord se trouve à Stark's Knob dans l'est de l'état de New York. Antérieurement rapportée comme une roche extrusive dans le faciès de pente et de pied de pente de l'Ordovicien allochtone, cette petite lentille (~ 125+ m long, 39 m épais) est en fait un bloc limité par des failles dans le mélange (Ordovicien supérieur) sous le chevauchement frontal taconien. Sa géochimie de basaltes médio-océaniques actuels normaux (N-MORB) et sa composition de spinelle sont caractéristiques des environnements de crête océanique à une profondeur de 2 km ou plus. D'abondantes lentilles de calcaire sur coussinets et les plates-formes de lave à l'intérieur des coussinets ont donné un gastropode datant de l'Ordovicien tardif. Les calcaires concordent avec cette profondeur d'extrusion et avec la production limitée de carbonate pélagique au Paléozoïque précoce par le transport de boue de chaux de la plate-forme laurentienne ou par la précipitation abiotique des carbonates lors du réchauffement de l'eau de mer durant l'extrusion du basalte. Une relation génétique est probable entre les basaltes parautochtones de Stark's Knob et les volcaniques allochtones de Jonestown dans le facies de pente et de pied de pente du klippe de Hamburg, dans l'est de la Pennsylvanie. Les deux sont des basaltes MORB de l'Ordovicien qui reflètent le volcanisme sur la pente de la fosse externe en subduction avant la collision entre l'arc taconique et la Laurentia. L'orogenèse taconique peut avoir conduit à la production de basalte sur la plaque en subduction en : (1) initiant du mouvement surtout coulissant, parallèle à l'orogène, sur la plaque en subduction, avec des basaltes MORB générés aux retraits dans un environnement analogue à celui du golfe de la Californie ou (2) en développant des failles dans un régime extensionnel induit par de la flexure. Par l'un ou l'autre des procédés, le volcanisme mafique semble être un processus rare mais tectoniquement significatif sur les pentes externes des fosses alors que les marges continentales ou les plaques océaniques entrent dans les zones de subduction.

[Traduit par la Rédaction]

Received 19 February 2003. Accepted 24 July 2003. Published on the NRC Research Press Web site at http://cjes.nrc.ca on 9 December 2003.

Paper handled by Associate Editor J.D. Greenough.

Ed Landing.[1] New York State Museum, Albany, NY 12230, U.S.A.
Georgia Pe-Piper. Department of Geology, Saint Mary's University, Halifax, NS B3H 3C3, Canada.
William S. F. Kidd. Department of Geological Sciences, State University of New York at Albany, Albany, NY 12222, U.S.A.
Karem Azmy. Mineralogisch-Petrographiches Institut, Universität Basel, Bernoullistrasse 30, CH-4056 Basel, Switzerland.

[1]Corresponding author (e-mail: elanding@mail.nysed.gov).

 doi: 10.1139/E03-076

Introduction

Stark's Knob is a small (30 m-high) volcanic body 5 km west of the frontal thrust of the Taconic allochthon in eastern Saratoga County, New York (Fig. 1). It lies 200 m west of the intersection of US Route 4 – NY Route 32 with Stark's Knob Road. Early quarrying removed the east side of the knob (Cushing 1914) and exposed a section through most of the pillow basalt.

Stark's Knob is the only pillow basalt in synorogenic sedimentary rocks on the exterior (western or northern) margin of the Middle–Late Ordovician Taconian orogen in the Appalachians (Fisher 1977; Williams 1979). Stark's Knob has been discussed in many publications (Woodward 1903; Cushing 1914; Urry 1936, p. 1225, table 1; Zen 1967, 1974; Bird 1968; Bird and Dewey 1970; Vollmer and Bosworth 1984) and field trip guides (Balk 1933; Hewitt et al. 1965; Landing 1988; Zen 1989; Kidd et al. 1995). However, its age and relationship to surrounding Ordovician siliciclastics has remained problematical. If Stark's Knob basalt extrusion was coeval with Taconian orogeny and on the Laurentian plate margin that was entering the east-dipping Taconic subduction zone (e.g., Bird and Dewey 1970; Zen 1989), this volumetrically minor basalt is tectonically significant. Modern outer trench-slope magmatism is unknown, although limited evidence (Hoffman 1987) suggests mafic magmatism occurs in this setting in early stages of some arc–continent or continent–continent collisions. We compare the Stark's Knob basalt with the Jonestown volcanics in eastern Pennsylvania and emphasize the importance of these extrusives as the only known volcanics in syncollisional Ordovician flysch and melange of the Appalachians. We suggest that mafic magmatism, although rare, is tectonically significant as continent margins or oceanic plates enter subduction zones.

Earlier work

Woodworth (1903) and Cushing (1914) correlated the Stark's Knob basalt with Late Triassic–Early Jurassic flows and intrusions elsewhere in the northeastern U.S. and regarded the limestones between the pillows as fragments of the underlying Cambrian–Ordovician carbonate platform. In contrast to this autochthonous interpretation, Fisher et al. (1970) and Fisher (1977) regarded Stark's Knob as extrusive in lower Upper Ordovician (Llandeil – lower Caradoc) slope-rise facies of the Mount Merino Formation and located Stark's Knob in the westernmost klippe of the Taconic allochthon. However, Landing (1988) noted that the Stark's Knob basalt is not in the Mount Merino (green siliciclastic mudstone and chert), but rather in black mudstone and turbiditic sandstone. This facies is comparable either to the overlying Austin Glen Formation (lower Caradoc; = "Pawlet Formation," see Landing 1988), the highest formation in the allochthon, or the middle Caradoc melange under the allochthon (Berry 1962, 1968).

If Stark's Knob is a melange block, then its age and tectonic significance are ambiguous. Blocks with a wide range in age (from Middle Proterozoic basement to fragments of the Taconic accretionary prism) and size (up to 10 km long) occur in Taconic melange (Zen 1967, pp. 35–40; Ratcliffe and Bahrami 1976). The only other pillow basalts in eastern New York are in the Lower Cambrian Rensselaer Formation in the Taconic allochthon (Balk 1953; Potter 1972). Derivation of Stark's Knob from the Rensselaer would mean it is an extrusive related to earliest Cambrian extension of the Laurentian margin and formation of the Iapetus Ocean (e.g., Bédard and Stevenson 1999). Thus, uncertainties in age (Cambrian or Ordovician), stratigraphy, and structural context (in situ, parautochthonous, or allochthonous) meant that work on biostratigraphy, limestone deposition, and basalt geochemistry could relate Stark's Knob to the early Paleozoic evolution of east Laurentia.

Geologic setting

Mapping of the Hudson River lowland north into Saratoga County shows that Stark's Knob is best interpreted as a block in the north-northeast-trending Cohoes melange west of the Taconic allochthon (Bosworth and Vollmer 1981; Vollmer and Bosworth 1984; Plesch 1994; Kidd et al. 1995; Fig. 1). The Cohoes melange is derived from synorogenic flysch dominated by lithic arenite ("graywacke") and mudrocks. Stark's Knob occurs within the thrust fault-bounded Mohawk River Central Zone of the Cohoes melange. Structurally disrupted dark mudstones and turbiditic sandstones of the melange are exposed to the south-southwest in roadcuts on Stark's Knob Road (Fig. 2).

The main body of Stark's Knob pillow basalt is a N20°W-striking, ca. 125 m-long lens (Fig. 2). Isolated basalt outcrops, 1–2 m in diameter, occur at the north end of the quarry (see Cushing 1914, fig. 13) and about 50 m southeast of the main volcanic body (Fig. 2). It is unclear if these blocks were emplaced by mass wasting of an olistolith or are structurally detached from the main basalt. No other basalt fragments are known in the Cohoes melange.

Faulted contacts of basalt pillows with melangy shales, including dark silty mudstone and thin turbiditic lithic sandstone, are exposed at the north end of the quarry and on the southwest slope of Stark's Knob. The mudrocks near these contacts show phacoidal fracturing and cleavage and structural disruption typical of the melange elsewhere in the area. Calcite slickensides occur at the base of the pillows on the east side of the quarry (Fig. 2, cross section). These features are consistent with faulted contacts with the pillow basalt. Thin sections of slickensides indicate steps in calcite fibers, and the obliquity of the fibers show that the basal fault on the east side of Stark's Knob has a west-northwest (ca. 290°–300°) shear direction and sense of local Taconian thrusts. The east-dipping fault on the west side of the knob is much steeper than the east-dipping fault on the east side of the knob (Fig. 2). As there is no indication of a major fold in the pillow basalt, this relationship suggests faults of two different ages. The shallower dipping fault with calcite slickensides is inferred to truncate an older, steeper fault on the west side (Fig. 2). Interpretation of faulted contacts and structural isolation of the Stark's Knob basalt are consistent with Cushing's (1914) and our observations of an absence of (1) baked contacts with the surrounding melange, (2) shale or arenite lenses or inclusions in the basalt, and (3) basalt intrusions in the flysch.

Dip is difficult to determine precisely across the basalt, but is nearly vertical on the east at a contact with steeply west-dipping flysch and decreases west to ca. 50°W on the knob's crest. The tops-sense of the pillow basalt is to the west. This evidence is recorded by reddened (baked) tops of

Fig. 1. Regional geological map showing location of Stark's Knob in the external melange and deformed flysch of the Taconic foreland basin (after Kidd et al. 1995; Hayman and Kidd 2002). Cities: A, Albany; G, Glens Falls; P, Saratoga Springs; S, Schenectady; T, Troy.

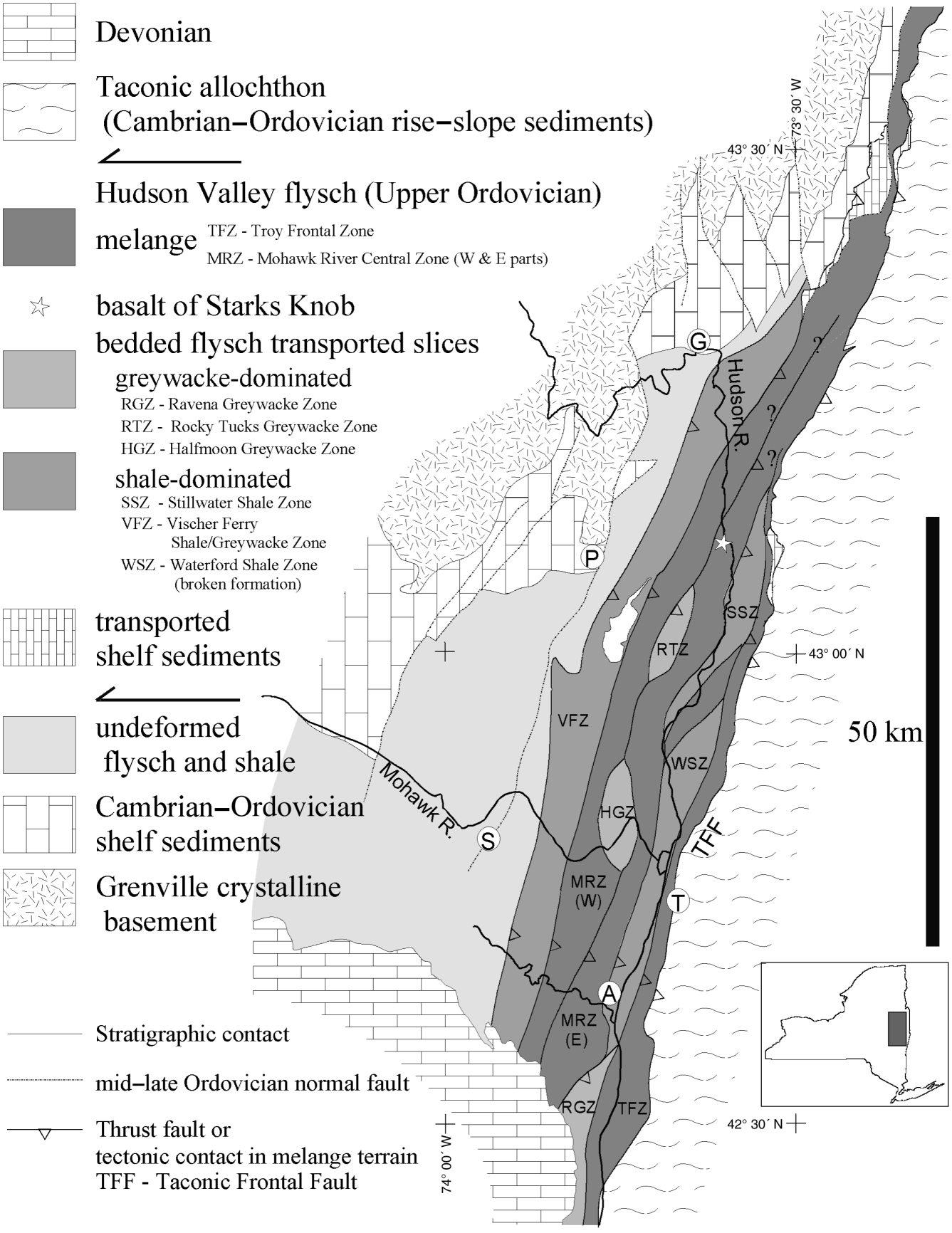

Fig. 2. Large scale geologic map and cross section of Stark's Knob. Mapping by W. Kidd using electronic total section. Contour intervals in feet (10 feet ≈ 3.048 m). ASL, above sea level.

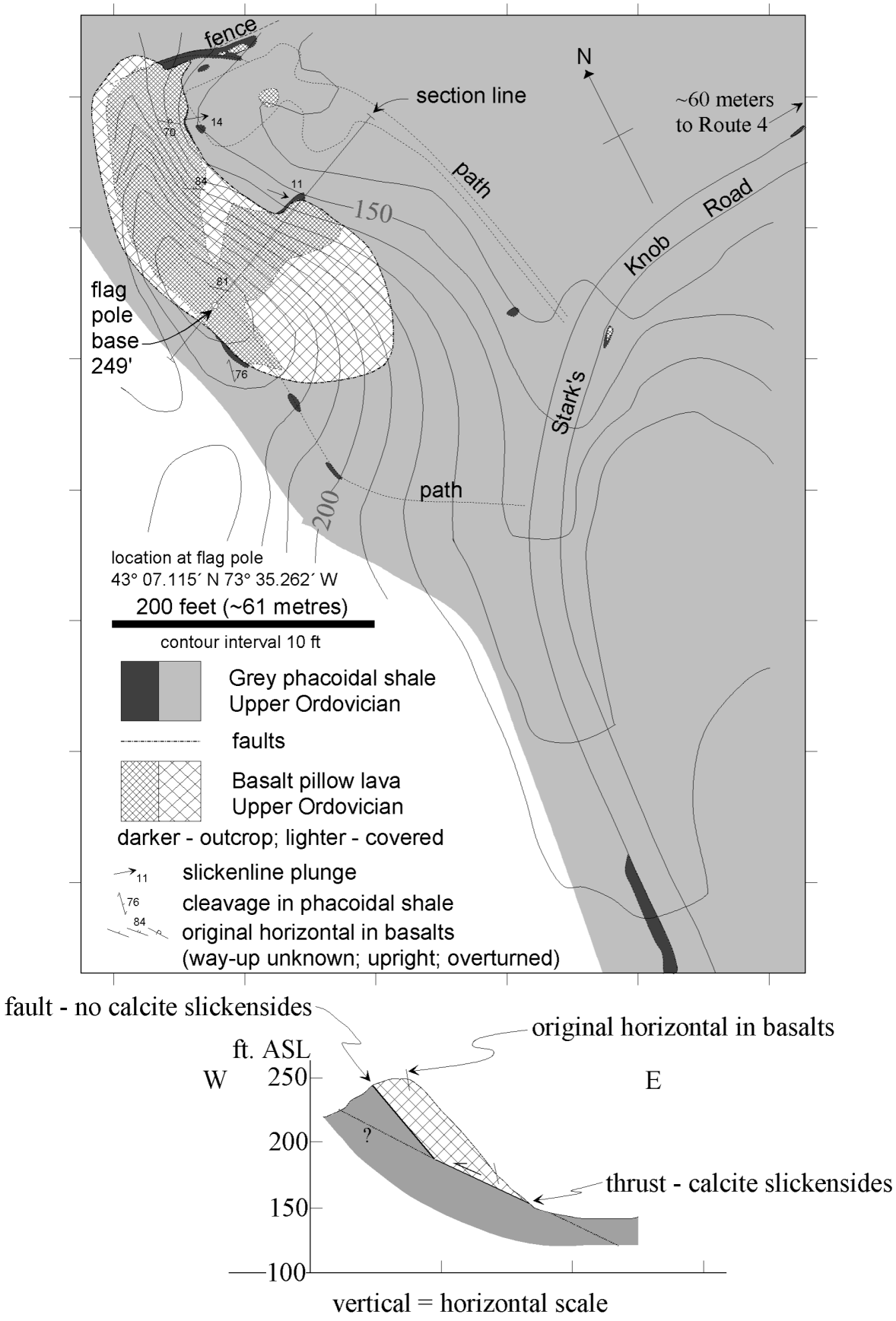

limestone lenses on the crest of the knob (Fig. 3*d*). Near the base of the quarry high wall and approximately half-way through the pillow basalt sequence, thin (1–3 cm), steeply east-dipping limestone lenses occur within several pillows (Fig. 3*c*). These limestones record deposition of fine-grained carbonate on lava shelves that formed when active lava tubes drained (Francheteau et al. 1980; Moore et al. 1985). Lava shelves are rare features considered to form in the upper part of lava tubes (Moore et al. 1985). However, their presence on the east side of the Stark's Knob pillows suggests that lava shelves can form in the lower part of a lava tube, and they provide ambiguous evidence for tops-sense. Presumption of a westerly top-sense throughout; absence of tight folding (noted earlier in the text), and steep, west-decreasing dip allow determination of a maximum, ca. 39 m thickness of pillow basalt, with the lower 12 m poorly exposed in the quarry floor.

The pillows are black, have scattered, small (ca. 0.5 mm diameter), calcite-filled amygdules throughout and are generally small (20–45 cm diameter, with a maximum cross section of 2.5 m × 1.0 m for a pillow 20 m northwest of the knob's crest). The exterior several centimetres of the pillows are greenish black, in places slickensided by rotation and shear of the pillows, and spall away with weathering. Fractures lined with white, sparry calcite and an internal fill of light grey, silt-size calcite cut the pillows in variable abundance. As these radial fractures rarely extend to the pillow margins (Fig. D1)[2], they are apparently related to quenching, and not tectonic shear.

With exception of in-faulted slivers of sheared, black silty mudstone at the exterior margins of the pillow basalt (Cushing 1914), the only non-basalt lithology at Stark's Knob is a light gray, white-weathering, fine-grained limestone. This limestone is common as short strings of thin-bedded fragments that adhere to the pillow margins. This disrupted habit may have locally resulted from rotation of the pillows and fracturing of a bedded limestone. Non-tectonized limestone lenses up to 25 cm thick fill depressions between extruded pillows on the crest of Stark's Knob (Fig. 3*d*). A second type of non-disrupted limestone is the lenticular carbonate on lava shelves in pillows in the lower part of the quarry (Fig. 3*c*). These limestones represent a carbonate that accumulated on lava shelves after the basalt was extruded as pillows (e.g., Francheteau et al. 1980).

Limestone age and deposition

The limestones offered a potential for refining biostratigraphic correlation and reconstructing the extrusion environment. Fifty-nine limestone samples were taken through the basalt succession, slabbed for sedimentary structures, cracked for macrofossils, and processed for acid-resistant microfossils.

Limestone petrography and deposition

Limestones were noted in the 16.5–39 m interval at Stark's Knob. Poor exposure likely obscures lower lenses. Thin sections show neomorphic, closely fitted, small (0.2–0.6 mm), equidimensional, anhedral–subhedral calcite crystals. These "pure limestones" (Cushing 1914, p. 120) produce < 0.05% siliciclastic residue after acid disaggregation for microfossils and minor opaque (organic?) material with carbonate geochemical processing. Planar lamination is the only primary structure (Fig. 3*d*); this feature is consistent with deposition of calcareous mud or silt under low wave or current energies prior to aggradational recrystallization. Sub- to well-rounded basalt fragments at the base of the lenses (Fig. 3*d*) suggest episodic or protracted, high-energy conditions before carbonate accumulation. Rapid deposition coeval with pillow extrusion is shown by reddened, baked tops of some lenses (Fig. 3*d*), corroded limestone inclusions in pillows (Cushing 1914, fig. 11), and limestone fills of multiple, 5–8 cm-high voids above lava shelves that developed in active lava tubes (Fig. 3*c*).

Biostratigraphy

Recovery of fossils from the limestone lenses was disappointing, in part because of the small samples available for processing (average 0.4 kg, but three 3.5 kg samples). A crinoid columnal and a trilobite sclerite were noted on limestone slabs. 36 kg of limestone from 46 sample horizons did not yield acid-resistant fossils.

A mold of a gastropod conch was recovered from a limestone (Figs. 3*a*, 3*b*). Although little detail is preserved, the three relatively rapidly expanding, convex whorls support reference to a few pre-Silurian gastropods with low turbiniform shells (e.g., Knight et al. 1960). Among these is *Leiospira* Ulrich and Scofield, 1897, a common genus in the middle Upper Ordovician Trenton Group and higher strata. Identification of *Leiospira*? sp. is important; it precludes derivation of the Stark's Knob pillow basalt from lowest Cambrian rift facies of the Rensselaer Formation in the Taconic allochthon.

Depositional setting

Abundant limestones suggest that relationships, other than structural proximity, of the Stark's Knob pillow basalt to the Mount Merino or Austin Glen – "Pawlet" Formations in the Taconic allochthon or to the parautochthonous Cohoes melange are unlikely. The slope–rise to fore-arc facies of these siliciclastic units lack limestone and are not intercalated with the pillows (Rowley et al. 1979). Westrop et al. (1995) detailed that early Paleozoic gastropods characterize near-shore – relatively shallow habitats. Thus, presence of *Leiospira*? sp., and pure limestones throughout Stark's Knob at a time in earth history without significant pelagic carbonate production has three potential explanations: (1) Volcanism and limestone deposition were shallow-marine, perhaps on a sea mount or shelf, (2) the snail and carbonate were transported into deep-water, or (3) carbonate production was in a deep-water(?) seep setting. Explanation (1) required analysis to determine approximate basalt extrusion depth (discussed later in the text). Explanation (2) is unlikely if the basalt is allochthonous, as the Mount Merino, Austin Glen, and Cohoes melange had an eastern sediment provenance in the Taconic orogen and consist of increasingly immature siliciclastic debris (e.g., Rowley

[2] Depository data can be purchased from the Depository of Unpublished Data, Document Delivery, CISTI, National Research Council of Canada, Ottawa, ON K1A 0S2, Canada. Depository data include Figs. D1 (Photograph of pillow basalt slab) and D2 (Backscatter electron images petrographic textures and mineral assemblages) and Tables D1 to D4.

Fig. 3. Limestones and gastropod from Stark's Knob. (*a*, *b*) *Leiospira*? Ulrich and Scofield, 1897; lateral (inclined 45°) and abapical views of exterior mold, × 6.0 and × 6.5, respectively, showing broadly convex whorls, NYSM 17044. (*c*) Limestone-capped lava shelves in pillow in lower Stark's Knob sequence; 7 cm lens cap for scale. (*d*) Slab of light gray, inter-pillow, neomorphic limestone lens, × 0.55; basalt pebbles at base, reddened ca. 1 cm-thick interval at top baked by overlying pillow; black lamina at top of slab is spalled from overlying pillow, NYSM 17043.

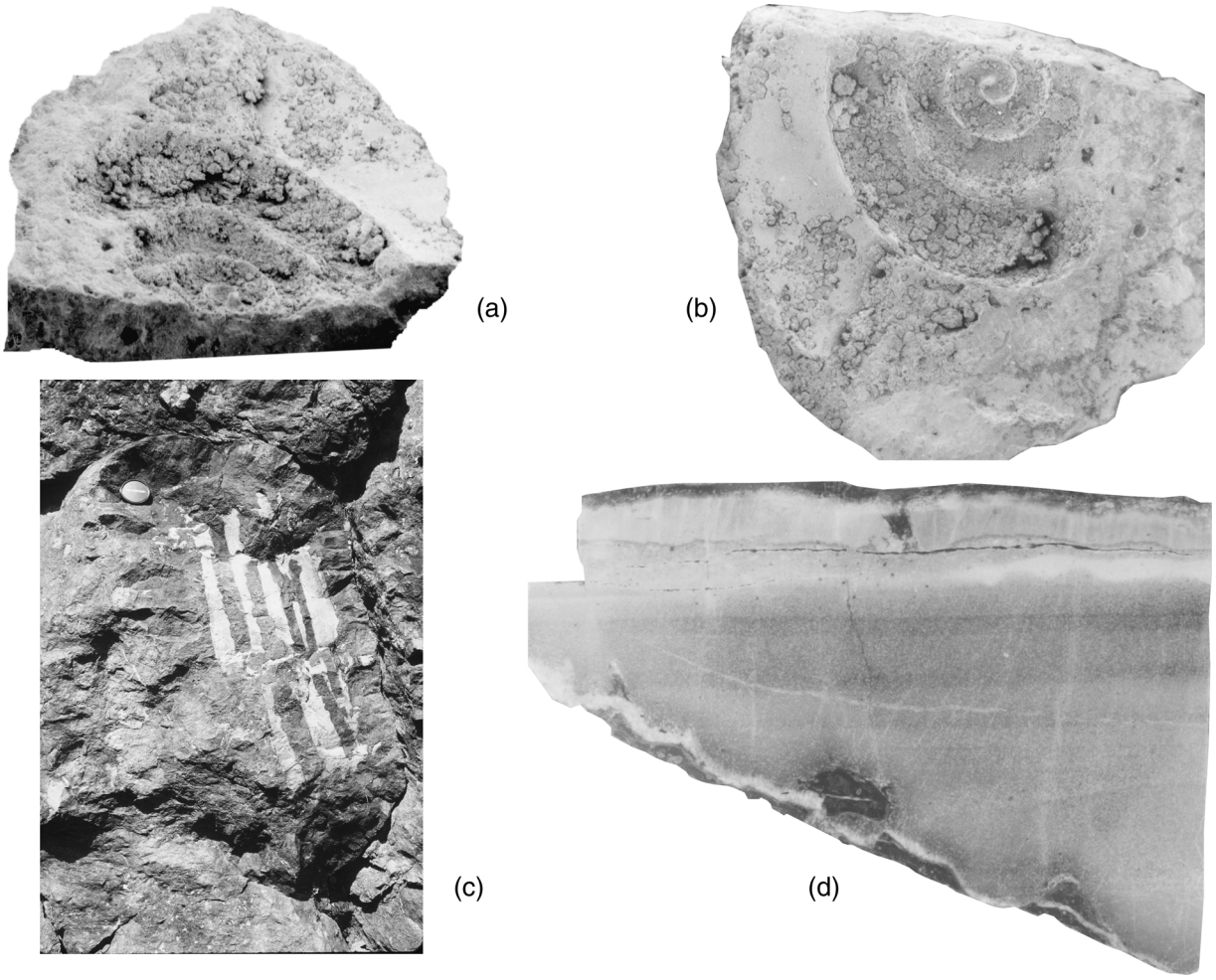

and Kidd 1981; Landing 1988). Thus, geologic setting mitigates against transport of lime mud or silt from the orogen and limestone deposition in a deep-marine setting. Explanation (2) is appropriate to carbonate transported from the Laurentian platform or to carbonate production and basalt extrusion at a site sheltered from sediments from the orogen. Explanation (3) required geochemical analysis.

Limestone geochemistry

Extrusion of Stark's Knob basalt during the Taconic orogeny suggested a relationship of its petrographically undistinctive limestone to the isotopically distinctive limestones at seeps (natural gas, brine, petroleum) on convergent margins and accretionary prisms (Kulm and Suess 1990). Seep limestones have highly negative $\delta^{13}C$ values, as opposed to the slightly positive values of limestones precipitated in equilibrium with seawater (e.g., Hoefs 1997). Trace elements and stable isotope geochemistry can also help reconstruct carbonate paleoenvironments (Azmy et al. 1998) and diagenesis (e.g., Al-Aasm and Azmy 1996). Chemical and isotopic signals of marine carbonates are dramatically changed by water–rock interaction (dissolution–precipitation) and help determine the diagenetic history of neomorphic limestones, as those at Stark's Knob. Some trace elements, such as Sr, are depleted in the secondary phase and in burial calcite cements, while others (e.g., Fe and Mn) are enriched (Veizer 1983*a*, 1983*b*; Tucker 1990). $\delta^{18}O$ values of secondary calcite are depleted relative to precursor marine carbonates, as the diagenetic fluid is usually meteoric water (Veizer 1983*a*, 1983*b*; Al-Aasm and Azmy 1994). $\delta^{18}O$ depletion is significant in deep-burial cements as high burial temperatures suppress ^{18}O–^{16}O fractionation during precipitation. However, $\delta^{13}C$ signals of burial cements may not be greatly altered if the diagenetic fluid contains little dissolved CO_2, as most of the $(CO_3)^{2-}$ comes from dissolution of the limestone, and there may be little ^{13}C–^{12}C fractionation with increasing burial temperature. Thus, $\delta^{13}C$ signals may reflect nearly original signatures of a precursor carbonate and distinguish marine or nonmarine origins.

Methodology

Four limestone samples were analyzed (Table 1), with two

analyses of sample SK 44 — SK 44 from the lower part of the lens and SK 44B from the baked top of the lens (Fig. 3*a*). Powdered 0.2 mg samples were heated at 380 °C under vacuum for 1 h to remove volatiles and then stored in a desiccator. They were reacted with anhydrous H_3PO_4 at 74 °C in a Finnigan Keil III Carbonate Device. Water and CO_2 produced by the reaction were cryogenically separated; pure CO_2 was analyzed with a Finnigan-MAT 252 isotope ratio mass spectrometer at the University of Iowa. The measurements were calibrated against a laboratory reference gas (LASIS). Analytical precision was better than ±0.1‰ for carbon and oxygen isotope ratios. Trace element analysis was performed by dissolving ca. 15 mg powder samples in dilute HNO_3. The aliquots were analyzed by Axiom ICP–MS (inductively coupled plasma – mass spectrometry) at the Harry Reid Center of the University of Nevada-Las Vegas, with analytical precision and accuracy in relative percent for the following elements: Ca (2.1, 1.9), Mg (3.5, 0.4), Sr (2.7, 0.2), Fe (2.1, 0.3) and Mn (1.4, 0.9).

Results

$\delta^{13}C$ isotopic values are slightly positive and consistent with carbonates deposited in equilibrium with sea water (Table 1). The analysis does not distinguish between the possibilities that the calcisiltite was derived from calcareous skeletons or was partly or primarily abiotic and resulted from precipitation with heating of sea water during basalt extrusion and pH reduction with decreased CO_2 solubility.

Trace element analyses show low concentrations of Sr (61–166 ppm) but higher concentrations of Fe (637–3010 ppm) and Mn (1100–2140 ppm) — values comparable with deep-burial cements (e.g., Dorobek 1987). The latter values agree with depleted $\delta^{18}O$ signals (–9.9‰ to –12.8‰ PDB) of Stark's Knob limestones (see Dorobek 1987; Al-Aasm and Azmy 1996). The evidence is that these are marine carbonates significantly altered during diagenesis by dissolution–precipitation processes during burial and production of neomorphic calcite.

Basalt petrology

Ten samples from well-formed pillows with thick, originally glassy, chilled margins and coarser grained cores (Fig. D1) were studied from polished thin sections, and chemical analyses were made of rims and cores (Table 2). All samples show almost complete loss of primary minerals, and have numerous veinlets of alteration minerals, but generally show good preservation of original textures including delicate quench textures, such as glass and skeletal crystals. Veinlets were removed from the samples prior to chemical analysis.

At the chilled margins, the glass/crystal ratio is about 3:1, and glass has suffered polygonal fracturing–fragmentation and devitrification to spherulites of albite and Fe-rich chlorite (Fig. D2*a*). The pillow interiors show pilotaxitic to hyalopilitic texture, with abundant plagioclase (now albite) laths, and pseudomorphs after olivine and clinopyroxene phenocrysts. The glass/crystal ratio is about 1:1. Opaque minerals make up 1%–3% of the cores, and consist mainly of oxides (rutile, altered magnetite); chalcopyrite (Fig. D2*c*); graphite (replacing phenocrysts); and rare, small crystals of chromian spinel. Olivine phenocrysts were replaced originally by calcite (Fig. D2*d*) that was later partly replaced by chlorite, and chlorite veinlets also cut the entire original crystals. Phenocrysts with clinopyroxene outlines have been replaced entirely by chlorite.

Table 1. Limestone stable isotope geochemistry.

Sample No.	$\delta^{13}C$ (PDB)	$\delta^{18}O$ (PDB)
SK 44	1.44	–12.76
SK 44B	0.72	–9.88
SK 50	0.65	–12.67
SK 51	0.08	–12.68
SK 52	2.42	–12.80

Note: Fifty-two limestones that cap pillows or lava shelves were processed for microfossils; geochemical analysis was done on five. SK 44 and SK 44B are the lower (gray) and upper (baked and red) parts of a lens (Fig. 3*d*) on pillows near top of the Stark's Knob succession. PDB, Peedee Belemnite.

Basalt geochemistry

Of the seven chemical analyses of both cores and rims of pillows, four show significant differences between core and rim, which suggest an alteration history that influenced the rims more than the cores with loss of Fe_2O_3, MgO, CaO, K_2O, Ba, and addition of SiO_2 and Na_2O. Abundances of elements such as Ca and Na (reflected in the ubiquitous occurrence of albite) indicate that even the cores have experienced severe alteration and the LOI (loss on ignition) of the cores is higher than that of the rims (Figs. 4*a*–4*c*, Table D1). MgO shows a general correlation with LOI (Fig. 4*c*) and SiO_2 increases with decreasing MgO (Fig. 4*d*). The elements Ti, Y, and to a lesser extent Nb and Zr (Figs. 4*e*, 4*f*) are fairly constant from core to altered rim, although one core sample has an anomalously high Nb content of 8 ppm (of uncertain origin). Rock nomenclature based on these immobile elements shows the samples are all of basalt to andesite composition (Fig. 5*a*).

The immobile elements can be used to reconstruct the eruptive setting by comparison with published discrimination diagrams (Fig. 5). The Stark's Knob analyses occupy a restricted compositional range, suggesting that they preserve magmatic signatures. All fall in the MORB (mid-oceanic ridge basalt) field, although in some cases this field overlaps with island-arc tholeiite (IAT) (Fig. 5*b*) or volcanic-arc basalt (VAB) (Fig. 5*e*). The abundance of Nb, which is generally stable under sea-floor alteration conditions (Ridley et al. 1994), shows that these rocks are neither IAT nor VAB.

The REE spectra of Stark's Knob pillow cores (Fig. 6*a*) have unfractionated heavy REE (HREE) abundances, and are strongly depleted in the light REE (LREE). In this respect, they are very similar to N-type MORB (normal mid-ocean ridge basalt; e.g., Wilson 1989; Sun and McDonough 1989), with the sample with the lowest silica content being the closest to original N-type MORB basalt (heavy line in Fig. 6*a*). REE patterns for the rims (Fig. 6*c*) show similar, LREE depletion, as do the cores, but they show some HREE enrichment relative to the cores, similar to that noted by

Table 2. Whole-rock chemical analyses of representative pillow basalt samples.

Sample No.:	SK0.0c	SK0.0m	SK1c	SK1.5c	SK1.5m	SK3m	SK14c	SK14m
Major elements (wt.%) by XRF								
SiO_2	48.51	56.87	56.37	49.32	57.16	60.54	50.87	51.20
TiO_2	0.88	0.87	0.90	0.92	0.92	0.91	0.90	0.92
Al_2O_3	17.94	17.94	19.05	18.61	18.23	18.77	18.76	19.11
Fe_2O_{3t}	7.17	5.19	4.17	6.69	4.91	2.15	9.23	9.48
MnO	0.14	0.06	0.05	0.11	0.07	0.06	0.07	0.07
MgO	4.22	2.78	2.20	4.05	2.84	1.06	4.46	4.61
CaO	4.90	2.60	2.64	4.96	2.48	2.46	2.82	2.46
Na_2O	5.03	8.34	7.70	5.77	8.20	9.13	6.62	6.68
K_2O	1.84	0.26	1.31	1.69	0.44	0.76	0.51	0.59
P_2O_5	0.09	0.02	0.08	0.10	0.04	0.07	0.16	0.11
L.O.I	8.31	4.40	4.39	8.30	4.59	3.15	5.34	5.29
Total	99.03	99.33	98.86	100.52	99.88	99.06	99.74	100.52
Trace elements (ppm) by XRF								
Ba	1597	265	545	1084	304	407	65	73
Rb	40	15	35	35	17	26	23	25
Sr	336	331	384	376	312	441	198	169
Y	22	22	22	24	26	24	22	22
Zr	61	52	57	66	55	63	50	51
Nb	8	3	2	2	3	3	2	2
Pb	b.d.	3	5	6	3	3	3	5
Ga	15	8	11	14	9	7	12	14
Zn	45	31	26	48	30	17	72	78
Cu	65	140	24	16	10	41	19	21
Ni	111	99	67	124	95	38	151	155
V	190	147	154	168	156	135	138	148
Cr	492	454	476	406	426	382	448	390
REE and selected trace elements (ppm) by INAA								
La	0.92	1.18	1.10	0.89	1.77	1.31	0.96	0.79
Ce	3.00	3.00	4.00	3.00	6.00	4.00	4.00	3.00
Nd	3.00	3.00	4.00	3.00	4.00	4.00	5.00	4.00
Sm	1.29	0.81	1.26	1.34	1.40	1.33	2.07	1.54
Eu	0.48	0.34	0.45	0.55	0.55	0.54	0.70	0.50
Tb	0.40	0.30	0.30	0.40	0.40	0.40	0.40	0.30
Yb	1.67	1.54	1.52	2.06	2.41	1.73	1.56	1.75
Lu	0.26	0.25	0.26	0.32	0.38	0.29	0.24	0.27
Co	31	21	15	32	21	9	30	31
Cs	1.10	0.60	1.60	1.50	0.70	1.40	1.60	1.80
Hf	1.10	0.90	0.90	1.20	1.20	0.90	0.90	0.90
Th	0.10	b.d.	b.d.	b.d.	b.d.	b.d.	b.d.	b.d.

Note: Sample designation (e.g., SK0.0 or SK14) is distance (in m) above base of Stark's Knob (SK) pillow succession. SKLB indicates loose blocks (LB) of pillows collected at base of quarry high wall. C, pillow core; m, pillow margin; b.d., below detection.

Analytical methods and precision summarized by Pe-Piper and Piper (1989). INAA, instrumental neutron activation analysis; XRF, X-ray fluorescence.

Ludden and Thompson (1979) in modern sea-floor basalts. Plots of trace elements from pillow cores normalized to primitive mantle (Fig. 6c) show strong enrichment in large-ion lithophile elements (LILE) and relatively flat distributions of high-field strength elements (HFSE).

The basalt alteration has been further interpreted with isocon plots (Fig. 7; see Grant 1986), which are graphical solutions of Gresen's (1967) equations for comparing metasomatic changes with least-altered equivalent rocks. Comparison of pillow cores with average N-MORB (Fig. 7*a*) show that a best-fit line can be drawn for Ti, which shows little variation, and Y, which along with the trivalent REE is particularly immobile during hydrothermal alteration (Ridley et al. 1994). This fit suggests that the processes that affected pillow cores resulted in significant Mg and Ca loss and significant gain in Si, Al, Na, and LILE, but with little change in Fe, Mn, Cr,

Fig. 4. Selected element variation plots for the Stark's Knob pillow basalt. LOI, loss on ignition.

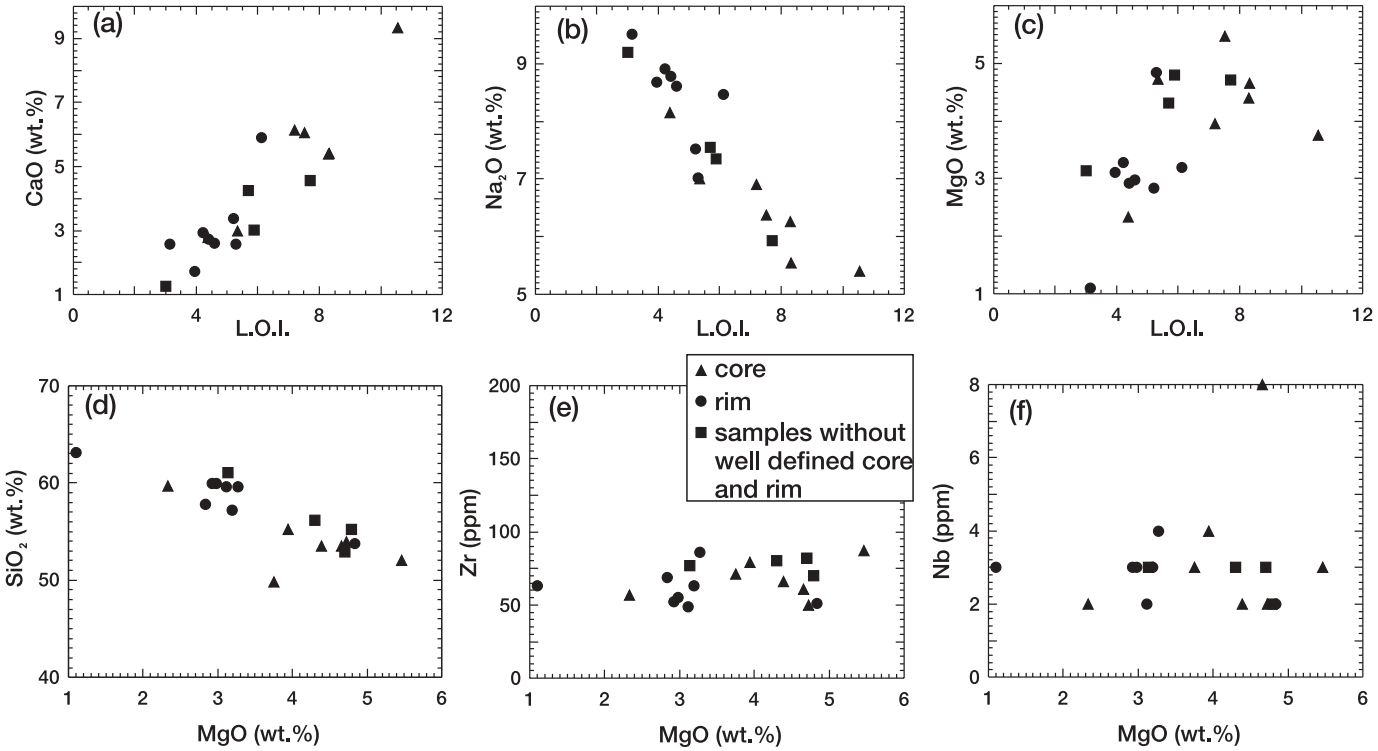

and P. In Fig. 7*b*, the least altered pillow core (SK0.0, Table 2) is compared with devitrified pillow rims. If Zr, Y, and, perhaps, Ti are immobile, then the rims show significant addition of Na compared with cores, no significant difference in Sr, and loss of Cr, P, Mg, Ca, Mn, Fe, and LILE. Si may show slight addition and Al slight depletion.

Chemical mineralogy

The only primary mineral preserved is rare spinel, which is picotite, a chromian spinel, with a low Cr/(Cr + Al) ratio (24:26) and Fe^{3+} content (0.04). Such low Cr/(Cr + Al) ratios are found only in some MORB lavas, being near the lower limit of these ratios in the MORB spinel compilation of Roeder (1994), and are not known in back-arc basin basalts (Dick and Bullen 1984; Pearce et al. 2000) (Fig. 8). The Fe^{3+} is also near the lower limit of Fe^{3+} reported by Roeder (1994) for MORB.

Albite (98%–100% Ab) and chlorite are ubiquitous alteration minerals. Chlorite after ferromagnesian phenocrysts is generally brunsvigite and contains small amounts of Cr (Table D4), whereas chlorite after groundmass glass or in veins is Cr-free pycnochlorite. Ripidolite and pseudothuringite with > 2% Cr have been analyzed from a pseudomorph after olivine and appear to replace an original chromite inclusion.

Rutile is the only oxide present. It occurs as small crystals in the groundmass or in small clots with limonite and chalcopyrite (Tables D2, D3). We used electron microprobe and X-ray diffraction to search for epidote, prehnite, smectites, and zeolites but these minerals were not found. "White mica" reported by Zen (1974, p. 236, 237) is consistent with our observations of small amounts of mica after feldspar, but was not further investigated.

Discussion

Basalt alteration history

Three basalt alteration phases are distinguished at Stark's Knob: (1) The vesicles and fractures were filled with calcite, which also replaced olivine, (2) the crystalline cores of the pillows, at least, were chloritized, and (3) the rims of the pillows were devitrified and further altered. Cooling fractures in pillows and early conversion of some ferromagnesian minerals to carbonate created substantial porosity, which was then filled during chloritization. Thereafter, significant porosity was present only at pillow margins, and some porosity may have developed by devitrification of glassy pillow rims.

The phase (1) of hydrothermal alteration compares with that of oceanic basalt remote from siliciclastic sediment (e.g., Staudigel et al. 1981), where Si is depleted during alteration and ferromagnesian minerals alter to calcite. The phase (2) chloritization of Stark's Knob pillows shows strong enrichment in Si, Al, and Na that is consistent with albite formation (67% SiO_2; 20% Al_2O_3; Table D4). Although some of the necessary Si and Al may have come from breakdown of ferromagnesian minerals, the isocon plot (Fig. 7*a*) suggests net enrichment of the pillows in both elements. Mg depletion is unexpected for chloritization reactions (chlorite 10%–18% MgO) and can be interpreted by an initial breakdown of ferromagnesian minerals to carbonates. Loss of Ca occurred with the petrographically observed replacement of calcite by chlorite. Petrographically, Fe–Ti oxides appear to have altered to rutile and limonite at Stark's Knob; the isocon plot suggests this change was essentially isochemical. The most likely source for Si and Al would be surrounding siliciclastic sediment; chert is ruled out as a source of Si, as it is not abundant in the Cambrian – Upper Ordovician of the Taconic allochthon

Fig. 5. Paleotectonic discriminant diagrams for Stark's Knob pillow basalt. Symbols as in Fig. 4. (*a*) Rock classification based on Zr, Y, Nb, and TiO_2 content (Winchester and Floyd 1977). (*b*) Zr/Y vs. Zr plot (fields after Pearce and Norry 1979). (*c*) Cr vs. Y plot (fields after Pearce 1982). (*d*) Plot of Nb × 2 – Zr/4 – Y (fields after Meschede 1986). (*e*) Ti/100 – Zr – Y × 3 plot (fields after Pearce and Cann 1973). Symbols as in Fig. 4.

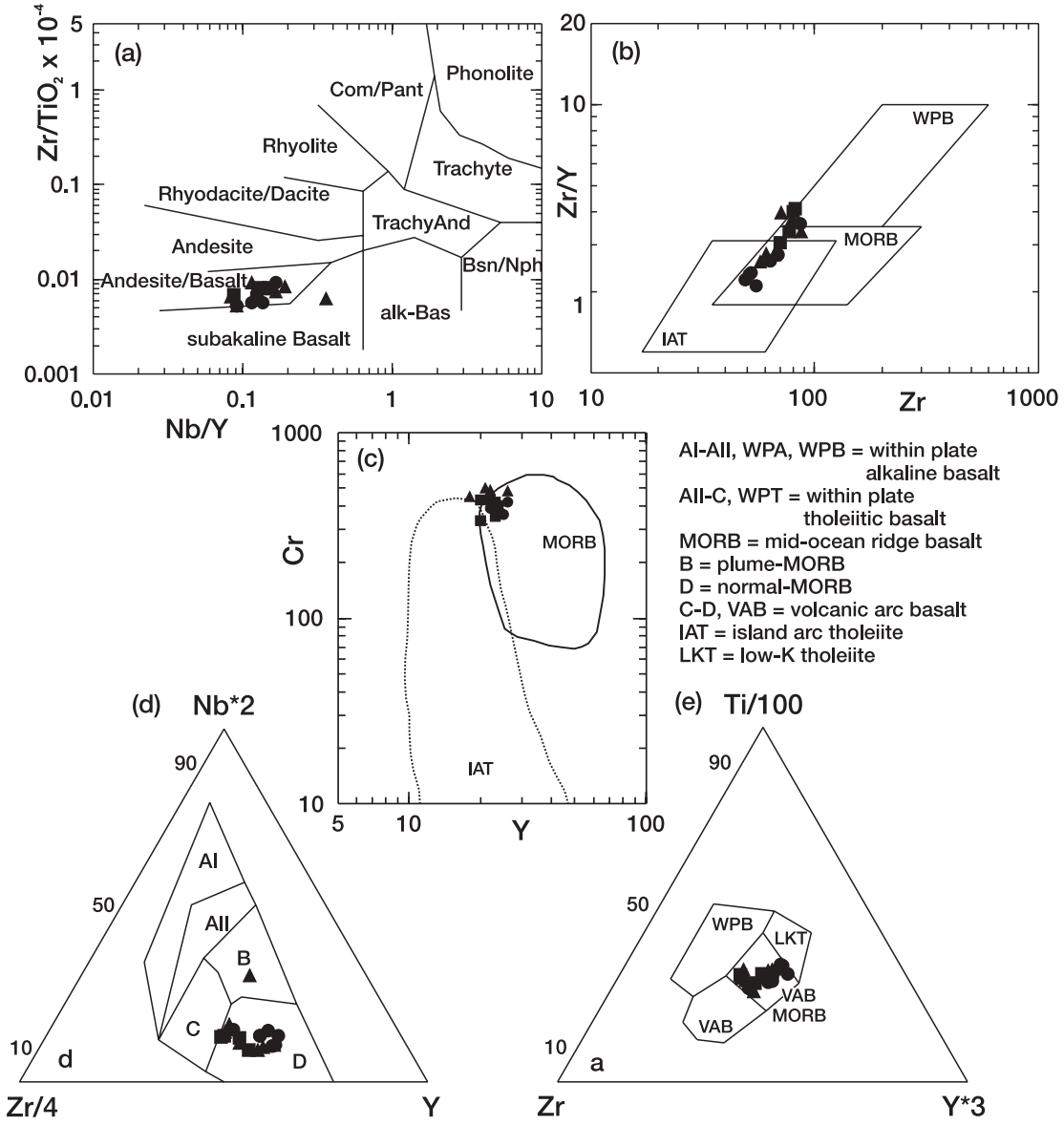

Fig. 6. (a) Chondrite-normalized rare-earth element (REE) pattern for pillow cores; (*b*) REE for pillow rims; (*c*) Spidergrams of primitive mantle-normalized trace element distributions in pillow cores. Normalizing factors from Sun and McDonough (1989). Symbols as in Fig. 4.

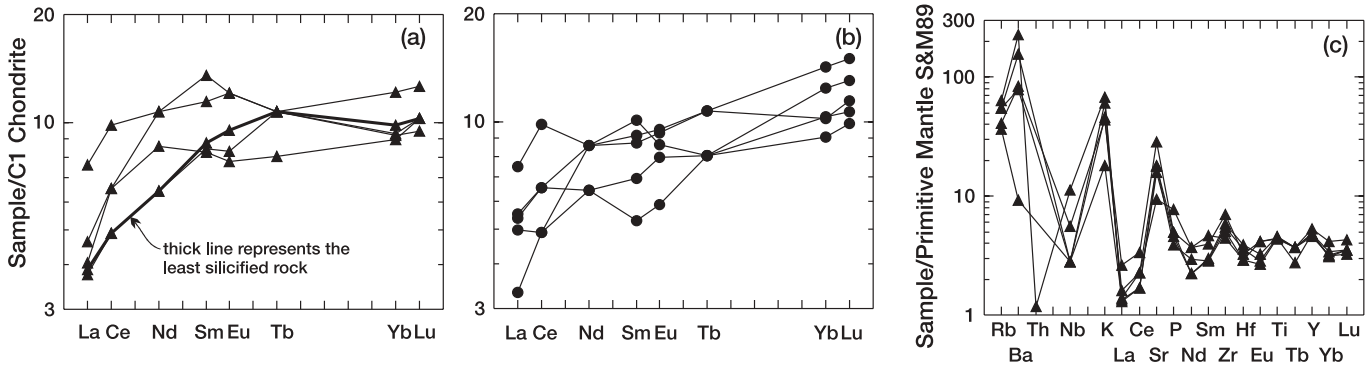

Fig. 7. Isocon diagrams (method of Grant 1986). (*a*) Concentration of major and trace elements from Stark's Knob pillow cores plotted against N-MORB element concentrations (see Sun and McDonough 1989 for trace elements, Schilling et al. 1983 for major elements). (*b*) concentration of elements in the least-altered pillow core SK0.0 plotted against element concentration in devitrified pillow rims.

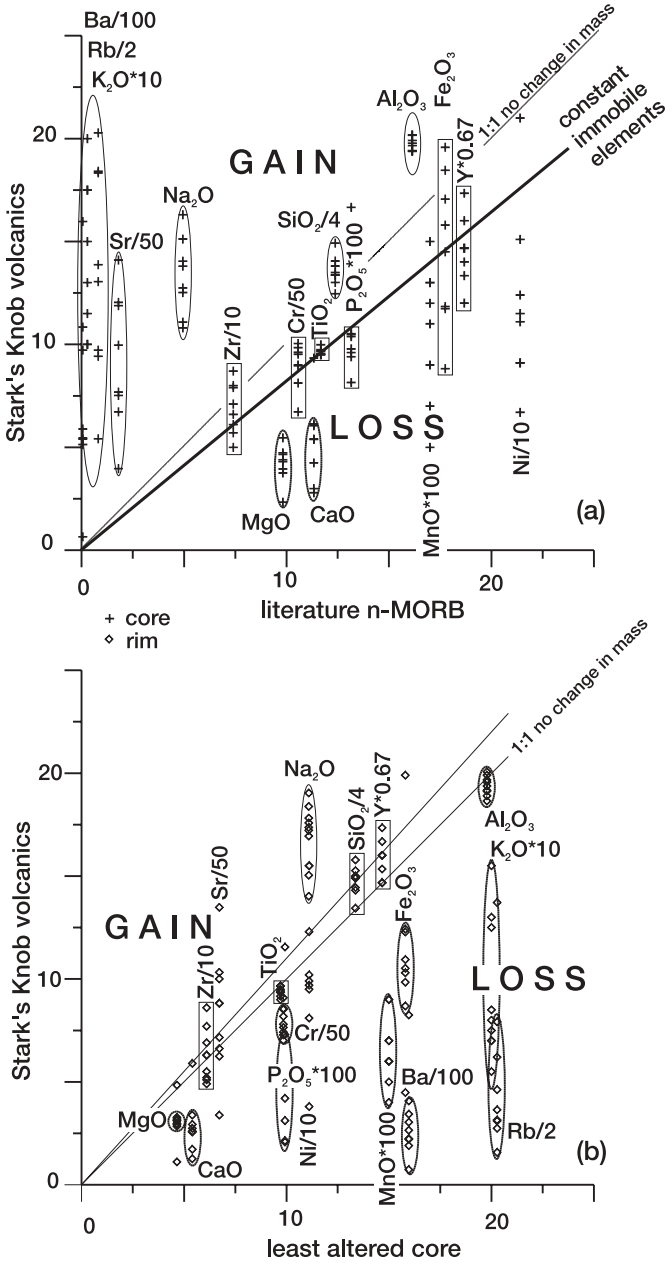

(e.g., Landing 1988) and is absent in the Cohoes melange. Similar hydrothermal alteration has been reported at ODP (Ocean Drilling Program) sites 857 and 858 (Stakes and Schiffman 1999), where MORB is buried by siliciclastic sediment near the Juan de Fuca ridge.

Pillow rim alteration involved loss of many elements. Where elements such as Mg or Ca are depleted in cores and rims on the isocon plots, it is difficult to assess which of the three alteration phases caused the depletion. However, compared with cores (Fig. 7*b*), the rims show significant loss of LILE, which are commonly flushed by circulating water. Fe and Mn, largely present in limonite in the cores, are substantially depleted, whereas Ti, largely in rutile in the cores, shows little

Fig. 8. Chemical variability in chromite from various tectonic environments (largely from Pearce et al. 2000) showing location of Stark's Knob samples (Table 3).

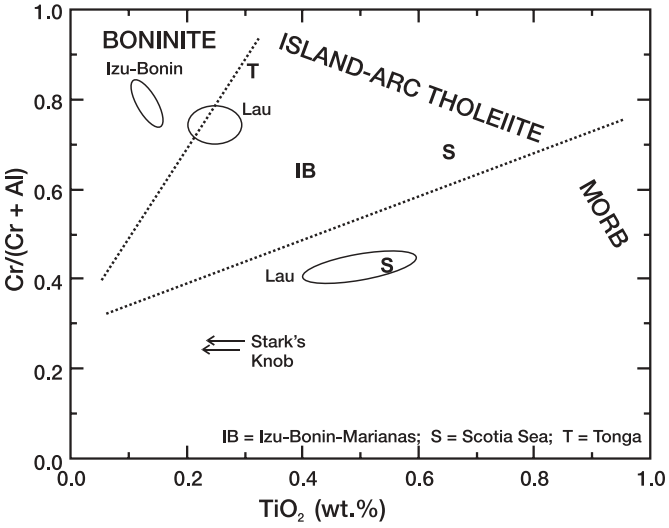

Table 3. Electron microprobe analyses of spinel (picotite) from loose block (LB) of Stark's Knob (SK) pillow basalt.

Sample No.:	SKLB1B	
Position:	4–1	4–2
SiO_2	0.30	0.37
Al_2O_3	44.03	45.28
FeO_t	13.40	13.27
MgO	18.62	18.80
CaO	0.17	b.d.
Cr_2O_3	23.49	22.29
Total	100.01	100.01
Atomic Formulae[a]		
Si	0.066	0.081
Al	11.407	11.659
Fe^{2+}	1.819	1.828
Fe^{3+}	0.718	0.676
Cr	4.081	3.849
Mg	6.107	6.128
Ca	0.04	b.d.
Mg#[b]	0.77	0.77
Cr#[b]	0.26	0.25
Fe3#[b]	0.04	0.04

[a]Total iron reported as FeO. Atomic formulae were calculated on the basis of 32 oxygens. Total iron as Fe^{3+} and Fe^{2+} was apportioned using the stoichiometric assumption: $2(Mg + Mn + Ca + Fe^{2+}) = (Cr + Al + Ti + Fe^{3+})$.

[b]Mg# = $Mg/(Fe^{2+} + Mg)$; Cr# = $Cr/(Cr + Al)$; Fe3# = $Fe^{3+}/(Fe^{3+} + Al + Cr)$.

depletion. Al is consistently slightly depleted compared with Si, and this relationship may be due to loss of Al or addition of Si. Decrease in LOI (Fig. 4) suggests devitrification of glass. Na is the only element to show major net addition in the rims. We suggest that the final rim alteration is consistent with devitrification and diagenesis involving low-temperature formation waters and slight silicification, although a sea-floor alteration process cannot be excluded.

In summary, Stark's Knob pillow alteration involved three phases. The first was conversion of some ferromagnesian minerals to carbonate (Fig. D2*d*), which increased porosity. This must have occurred before burial in siliciclastic sediment. We suggest that this type of sea-floor alteration took place with hydrothermal circulation through the basalt and associated carbonate-rich sediment, as proposed on the modern sea floor by Staudigel et al. (1981). The second phase involved porosity filling by development of chlorite (Fig. D2*e*) and albite by hydrothermal circulation that passed through siliciclastic sediment. This implies that siliciclastic sedimentation was essentially coeval with ocean-ridge processes and eventually buried the ridge basalts. The third stage involved devitrification of pillow rims and their alteration by cool circulating water. The timing of this phase is unknown, although it may have occurred after the overrunning of the Stark's Knob basalt lens by the Taconic master thrust. If so, it may have included conversion of original smectite to illite and resulting release of water.

Tectonic setting of Stark's Knob basalt

The Stark's Knob pillow basalt is not referable to the long-transported (ca. 75 + km) frontal slices of the Taconic allochthon (e.g., Zen 1967) but rather to the Cohoes melange under the Taconic master thrust. Interpretations of this basalt as a flow within the Taconic allochthon (Fisher et al. 1970; Fisher 1977) may have been based on Cushing and Ruedemann's (1914, p. 92) report of the graptolite *Didymograptus saggitarius* Hall, 1847, from "beds abutting at the north and south against" Stark's Knob. However, recovery of a graptolite known in the allochthonous Mount Merino and lower Austin Glen Formations is not relevant to determining the age, stratigraphy, or structural context of Stark's Knob. Cushing and Ruedemann's (1914) map shows the northern graptolite locality 100 m north of Stark's Knob in complex melange that also has a 2.0 km-long, lowest Ordovician block. The southern graptolite locality is not plotted on Cushing and Ruedemann's (1914) map and may be from an older block in the Cohoes melange.

The snail *Leiospira*? sp. shows that limestone deposition and pillow extrusion correlate with the middle Upper Ordovician Trenton Group and are younger than the highest unit (lower Upper Ordovician Austin Glen Formation) of the Taconic allochthon (see Mitchell et al. 1997 for new international definition of the Middle–Upper Ordovician boundary).

The abundant, nearly siliciclastic-free limestone lenses on and within the pillows and occurrence *of Leiospira*? are not consistent with the easterly provenance of synorogenic flysch (e.g., Rowley et al. 1979). Alternative explanations of shallow-marine carbonate production on Laurentia and carbonate transport to the east or abiotic carbonate production in sea water heated by basalt extrusion in a setting protected from siliciclastic input can explain the limestone lenses. Interior and shallower parts of the Laurentian margin were sites of Trenton Group carbonate production early in the Taconian orogeny, until carbonate production ended with transport of orogen-derived detritus across the platform. Thin, Trenton-equivalent sandstones with mollusk-rich faunas persist in synorogenic flysch that became the Cohoes melange on the meridian of Stark's Knob in the Hudson River valley (Ruedemann 1912). Continued carbonate deposition on the Laurentian margin into the early stages of the Taconian orogeny provides a western source for the limestones on the Stark's Knob pillows.

Tectonic interpretation of the Stark's Knob basalt must be consistent with igneous geochemistry. Immobile elements and stable minerals indicate extrusion as N-MORB in an ocean-ridge setting. This is emphasized by abundance of Zr, Ti, and Y (Fig. 5), REE distribution (Fig. 6), and presence of chromian spinel with a low Cr/Al ratio (Fig. 8).

Occurrence of limestones and fossils between the pillows and preservation of original pillow textures suggest a comparison with modern ocean ridges where basalts are extruded into relatively shallow environments associated with pelagic carbonates. The caveats to this comparison are the facts that important early Paleozoic pelagic carbonate sources are unknown and that abiotic carbonate production by sea water heating during pillow extrusion is an alternative explanation of the inter- and intra-pillow limestones.

Adjacent mudrock and sandstone at Stark's Knob suggest that the basalts were buried by and (or) tectonically incorporated into siliciclastics. These sediments likely supplied the Si and Al required to develop albite by hydrothermal alteration. The depth of extrusion associated with most modern MORB basalts is about 2 km or more, as on the modern Juan de Fuca ridge (Saunders et al. 1982; Fouquet et al. 1998). This further emphasizes that the Stark's Knob limestones are best interpreted as derived from the Laurentian shelf or abiotically produced.

Comparison with Jonestown volcanics

The Ordovician Jonestown volcanics of eastern Pennsylvania (Lash 1986) crop out in the allochthonous Hamburg klippe and occupy similar paleogeographic and temporal relationships to the parautochthonous Stark's Knob basalt. In the Hamburg klippe, basalt flows and subvolcanic intrusions are interbedded with deep-water siliceous mudstones and are overlain by turbidites. Chemical analyses of Jonestown basalts (although not as detailed as in our study) suggest a MORB origin. Lash (1986) proposed that the Jonestown volcanic–sedimentary association resulted from the encounter of a spreading ridge or a leaky transform fault with a trench (i.e., a setting similar to the subducting Juan de Fuca plate).

The Jonestown volcanics and the Stark's Knob basalt are MORB-type volcanics. In addition, both volcanics are associated with limestones (albeit the Hamburg klippe limestones are bedded and occur in older, late Early Ordovician rocks under the Jonestown volcanics). Both volcanic deposits were covered by siliciclastics after extrusion, as shown by the stratigraphic relationships of the Jonestown volcanics and the type of alternation of the Stark's Knob basalts. A cratonic source of siliciclastics that buried the Jonestown volcanics has been suggested (Lash 1989). The difficulty with this suggestion is that the coarser grained Middle Ordovician and younger siliciclastics that appear in the Taconian allochthons and

spread across the Laurentian margin were derived from the Taconic orogen (Rowley and Kidd 1981; Landing 1988).

Similarities in eruptive history, composition, and burial history point to a common origin of the Stark's Knob and Jonestown basalts and indicate formation of MORB basalt shortly before significant deposition of Late Ordovician siliciclastics. MORB basalt of this type is thus unrelated to the much older (Early Cambrian) rifting of Iapetus (e.g., Bédard and Stevenson 1999) and must have been produced and erupted during complex plate interations with subduction of the Laurentian margin beneath the Taconic arc. We hypothesize that arc–craton collision in the Taconic orogen led to basalt production on the subducting plate by two possible mechanisms. By the first, the transfer of motion from subduction to strike-slip led to formation of short en-echelon spreading centers and development of small ocean basins in a predominantly strike-slip setting. This first model has modern analogs in the Gulf of California (Saunders et al. 1982). A second, more hypothetical explanation for Stark's Knob basalt eruption does not require formation of small spreading centers in a strike-slip setting. By this process, deep faults develop with extensional flexing and faulting as a plate is forced into a subduction zone (see Bradley and Kidd 1991), and may lead to eruption of basalt through the subducting plate.

Acknowledgments

Support from the New York State Museum (NYSM), Albany, New York, and a Canadian Natural Sciences and Engineering Research Council of Canada grant to G. Pe-Piper is acknowledged. S. Ingram and E. Rutnick assisted with the figures. *Leiospira*?, collected during a SUNY-Albany geology class field trip, was evaluated by E.L. Yochelson (personal communication, 1986). W. Samsonoff provided access to scanning microscopy at the Wadsworth Center for Laboratories, New York State Health Department, Albany, New York. Illustrated specimens are reposited in the NYSM.

References

Al-Aasm, I.S., and Azmy, K. 1996. Diagenesis and evolution of microporosity of Middle-Upper Devonian Kee Scarp Reefs, Norman Wells, Northwest Territories, Canada: petrographic and geochemical aspects. American Association of Petroleum Geologists Bulletin, **80**: 82–100.

Azmy, K., Veizer, J., Bassett, M., and Copper, P. 1998. Oxygen and carbon isotopic composition of Silurian brachiopods: implications for coeval seawater and glaciations. Geological Society of America Bulletin, **110**: 1499–1512.

Balk, R. 1933. The Adirondack Mountains. 16th International Geological Congress, Guidebook 1, Excursion A-1.

Balk, R. 1953. Structure and graywacke areas and Taconic range east of Troy, New York. Geological Society of America Bulletin, **64**: 811–864.

Bédard, J.H., and Stevenson, R. 1999. The Caldwell Group lavas of southern Quebec: MORB-like tholeiites associated with the opening of Iapetus Ocean. Canadian Journal of Earth Sciences, **36**: 999–1019.

Berry, W.B.N. 1962. Stratigraphy, zonation, and age of Schaghticoke, Deepkill, and Normanskill shales, eastern New York. Geological Society of America Bulletin, **73**: 695–713.

Berry, W.B.N. 1968. Ordovician paleogeography of New England and adjacent areas based on graptolites. *In* Studies of Appalachian geology: northern and maritime. *Edited by* E. Zen, W.S. White, J. B. Hadley, and J.B. Thompson Jr. Interscience Publishers, New York, pp. 23–34.

Bird, J.M. 1968 Middle Ordovician gravity sliding—Taconic region. *In* North Atlantic: geology and continental drift. *Edited by* Kay, M. American Association of Petroleum Geologists, Memoir 12, pp. 670–686.

Bird, J.M., and Dewey, J.F. 1970. Lithosphere plate – continental margin tectonics and the evolution of the Appalachian orogen. Geological Society of America Bulletin, **81**: 1031–1059.

Bosworth, W., and Vollmer, F.W. 1981. Structures of the medial Ordovician flysch of eastern New York: deformation of synorogenic deposits in an overthrust environment: Journal of Geology, **89**: 551–568.

Bradley, D.C., and Kidd, W.S.F. 1991. Flexural extension on the outer trench slope of collisional foredeeps. Geological Society of America Bulletin, **103**: 1416–1438.

Cushing, H.P. 1914. The Northumberland volcanic plug. *In* Geology of Saratoga Springs and vicinity. *Edited by* H. P. Cushing and R. Ruedemann. New York State Museum Bulletin 169, pp. 115–135.

Cushing, H.P., and Ruedemann, R. 1914. Geology of Saratoga Springs and vicinity. New York State Museum Bulletin 169.

Dick, H.J.B., and Bullen, T. 1984. Chromian spinel as a petrogenetic indicator in abyssal and alpine-type peridotites and spatially associated lavas. Contributions to Mineralogy and Petrology, **86**: 54–76.

Dorobek, S.L. 1987. Petrography, geochemistry, and origin of burial diagenetic facies, Siluro-Devonian Helderberg Group (carbonate rocks), central Appalachians. American Association of Petroleum Geologists Bulletin, **71**: 492–514.

Fisher, D.W. 1977. Correlation of the Hadrynian, Cambrian, and Ordovician rocks of New York State. New York State Museum, Map and Chart Series, No. 25, 75 p.

Fisher, D.W., Isachsen, Y.W., and Richard, L.V. 1970. Geologic map of New York State, 1970, Hudson–Mohawk sheet. New York State Museum, Map and Chart Series, No. 15.

Fouquet, Y., Zierenberg, R.A., and Miller, D.J. 1998. Proceedings of the Ocean Drilling Program, Initial reports, Leg 169. College Station, Texas, Ocean Drilling Program.

Francheteau, J., Needham, D., Juteau, T., and Rangin, C. 1980. Naissance d'un ocean sur la dorsale du Pacifique Est—CYAMEX. CNEXO, Paris, France.

Grant, J.A. 1986. The isocon diagram: A simple solution to Gresen's equation for metasomatic alteration. Economic Geology, **81**: 1976–1982.

Gresens, R.L. 1967. Composition–volume relationships of metasomatism. Chemical Geology, **2**: 47–55.

Hayman, N.W., and Kidd, W.S.F. 2002. Reactivation of pre-thrusting, synconvergence normal faults as ramps within the Ordovician Champlain–Taconic thrust system. Geological Society of America Bulletin, **114**: 476–489.

Hewitt, P.C., McClellan, W.E., and Nilsson, H. 1965. Stop 3, Stark's Knob. *In* Guidebook for field trips. *Edited by* P. C. Hewitt and L. M. Hall. New York State Geological Association, 37th Annual Meeting, Union College, Schenectady, N.Y., pp. D10–D13.

Hoefs, J. 1997. Stable Isotope Geochemistry. Springer-Verlag, Berlin, Germany,208 p.

Hoffman, P.F. 1987. Early Proterozoic foredeeps, foredeep magmatism, and Superior-type iron-formations of the Canadian Shield. *In* Proterozoic lithospheric evolution. *Edited by* A. Kroner. American Geophysical Union, Geodynamics Series, 17, pp. 85–98.

Kidd, W.S.F., Pleach, A., and Vollmer, F.W. 1995. Lithofacies and structure of the Taconic flysch, melange and allochthon, in the

New York Capital District. *In* Field trip guide for the 67th Annual Meeting of the New York State Geological Association, Union College, Schenectady, New York. *Edited by* J.I. Garver and J.A. Smith. pp. 57–80.

Knight, J.B., Cox, L.R., Keen, A.M., Batten, R.L., Yochelson, E.L., and Robertson, R., 1960. Systematic descriptions. *In* Treatise on invertebrate paleontology, Part I, Mollusca 1. *Edited by* R. C. Moore. Geological Society of America and University of Kansas Press, pp. I171–I331.

Kulm, L.D., and Suess, E. 1990. Relationship between carbonate deposits and fluid venting: Oregon accretionary prism. Journal of Geophysical Research, **95**: 8899–8915.

Landing, E. 1988. Depositional tectonics and biostratigraphy of the western portion of the Taconic allochthon, eastern New York State. *In* The Canadian paleontology and biostratigraphy seminar—proceedings of meeting, Albany, N.Y., September 26–29, 1986. *Edited by* E. Landing. New York State Museum Bulletin 462, pp. 96–110.

Lash, G.G. 1986. Sedimentologic and geochemical evidence for Middle Ordovician near-trench volcanism in the central Appalachian orogen. Journal of Geology, **94**: 91–107.

Lash, G.G. 1989. Oceanic ridge subduction: a possible causal mechanism for sediment accretion. *In* Critical aspects of the plate tectonics theory, Vol. I. *Edited by* A.A. Augustithis. Theophrastus Pubs. S.A., Athens, Greece, pp. 291–303.

Ludden, J., and Thompson, G. 1979. An evaluation of the behavior of rare earths during the weathering of rare earth elements during the weathering of sea-floor basalt. Earth and Planetary Science Letters, **43**: 85–92.

Meschede, M. 1986. A method of discrimination between different types of mid-ocean ridge basalts and continental tholeiites with the Nb–Zr–Y diagram. Chemical Geology, **56**: 207–218.

Mitchell, C.E., Chen X., Bergström, S.M., Zhang, Y.-d., Wang, Z.-h., Webby, B.D., and Finney, S.C. 1997. Definition of a global boundary stratotype for the Darwillian Stage of the Ordovician System. Episodes, **20**: 158–166.

Pearce, J.A. 1982. Trace element characteristics of lavas from destructive plate boundaries. *In* Andesites. *Edited by* R. S. Thorpe, R.S. Wiley Interscience, Inc., New York, pp. 525–548.

Pearce, J.A., and Cann, J.R. 1973. Tectonic setting of basic volcanic rocks determined using trace element analyses. Earth and Planetary Science Letters, **19**: 290–300.

Pearce, J.A., and Norry, M.J. 1979. Petrogenetic implications of Ti, Zr, Y and Nb variations in volcanic rocks. Contributions to Mineralogy and Petrology, **69**: 33–47.

Pearce, J.A., Barker, P.F., Edwards, S.J., Parkinson, I.J., and Leat, P.T. 2000. Geochemistry and tectonic significance of peridotites from the South Sandwich arc–basin system. Contributions to Mineralogy and Petrology, **139**: 36–53.

Pe-Piper, G., and Piper, D.J.W. 1989. The Upper Hadrynian Jeffers Group, Cobequid Hills, Avalon Zone of Nova Scotia. Geological Society of America Bulletin, **101**: 364–376.

Plesch, A. 1994. Structure and tectonic significance of deformed medial Ordovician flysch and melange between Albany and Saratoga Lake and in the central Hudson Valley, New York. Unpublished M.Sc. thesis, State University of New York-Albany.

Potter, D.B. 1972. Stratigraphy and structure of the Hoosick Falls area, New York–Vermont, east-central Taconics. New York State Museum, Map and Chart Series, No. 19.

Ratcliffe, N.M., and Bahrami, M. 1976. The Chatham fault: A reinterpretation of the contact relationships between the Giddings Brook and Chatham slices of the Taconic allochthon in eastern New York. Geology, **4**: 56–60.

Ridley, W.I., Perfit, M.R., Jonasson, I.R., and Smith, M.F. 1994. Hydrothermal alteration in ocean ridge volcanics: a detailed syudy at the Galapagos fossil hydrothermal field. Geochimica et Cosmochemica Acta, **58**: 2477–2494.

Roeder, P.L. 1994. Chromite from the fiery rain of chondrules to the Kilauea Iki lava lake. Canadian Mineralogist, **32**: 729–746.

Rowley, D.B., and Kidd, W.S.F. 1981. Stratigraphic relationships and detrital composition of the medial Ordovician flysch of western New England: Implications for the tectonic evolution of the Taconic orogeny. Journal of Geology, **89**: 199–218.

Rowley, D.B., Kidd, W.S.F., and Delano, L.L. 1979. Detailed stratigraphic and structural features of the Giddings Brook slice of the Taconic allochthon in the Granville area. *In* Guidebook for field trips: Troy, New York, *Edited by* G. F. Friedman. New York State Geological Association 51st Annual Meeting and New England Intercollegiate Geological Conference 71st Annual Meeting, pp. 186–242.

Ruedemann, R. 1912. The Lower Siluric shales of the Mohawk valley. New York State Museum Bulletin 162.

Saunders, A.D., Fornari, D.J., Joron, J.-L., and Treuil, M. 1982. Geochemistry of basic igneous rocks, Gulf of California, Deep Sea Drilling Project, Leg 64. Initial Reports DSPD, 64, pp. 595–642.

Schilling, J.-C, Zapac, M., Evans, R., Johnston, T., White, W., Devine, J.D., and Kingsley, R. 1983. Petrologic and geochemical variations along the Mid-Atlantic Ridge from 27°N to 73°N. American Journal of Science, **283**: 510–586.

Stakes, D.S., and Schiffman, P. 1999. Hydrothermal alteration within the basement of the sedimented ridge environment of Middle Valley, northern Juan de Fuca Ridge. Geological Society of America Bulletin, **111**: 1294–1314.

Staudigel, H., Hart, S.R., and Richardson, S.H. 1981. Alteration of the oceanic crust: processes and timing. Earth and Planetary Science Letters, **52**: 311–327.

Sun, S., and McDonough, W.F. 1989. Chemical and isotopic systematics of oceanic basalts: implications for mantle composition and processes. *In* Magmatism in the ocean basins. *Edited by* A.D. Saunders and M.J. Norry. Geological Society (of London), Special Publication 42, pp. 313–345.

Ulrich, E.O., and Schofield, W.H. 1897. The Lower Silurian Gastropoda of Minnesota. Minnesota Geological Survey Bulletin, **3**: 813–1081.

Urry, W.B. 1936. Ages by the helium method: II Post-Keeweenawan. Geological Society of America Bulletin, **47**: 1217–1234.

Veizer, J. 1983*a*. Chemical diagenesis of carbonates: theory and application of trace element technique. *In* Stable isotopes in sedimentary geology. *Edited by* M.A. Arthur, T.F. Anderson, I.R. Kaplan, J. Veizer, and L.S. Land. Society of Economic Paleontologists and Mineralogists, Short Course Notes, No. 10, pp. III-1–III-100.

Veizer, J. 1983*b*. Trace elements and isotopes in sedimentary carbonates. Reviews in Mineralogy, **11**: 265–300.

Vollmer, F.W., and Bosworth, W. 1984. Formation of melange in a foreland basin overthrust setting: example from the Taconic orogen. Geological Society of America Special Paper, No. 198, pp. 53–70.

Westrop, S.R., Trembley, J.V., and Landing, E. 1995. Declining importance of trilobites in Ordovician nearshore communities: dilution or displacement. Palaios, **10**: 75–79.

Williams, H. 1979. Tectonic lithofacies map of the Appalachian orogen. Memorial University of Newfoundland, Department of Geology, Map 1.

Wilson, M. 1989. Igneous Petrogenesis: A Global Tectonic Approach. Unwin Hyman, London.

Winchester, J.A., and Floyd, P.A. 1977. Geochemical discrimination of different magma series and their differentiation products using immobile elements. Chemical Geology, **20**: 325–343.

Woodworth, J.B. 1903. The Northumberland volcanic plug. New York State Museum, 21st Report of the State Geologist 1901, pp. r17–r29.

Zen, E. 1967. Time and space relationships of the Taconic allochthon and autochthon. Geological Society of America, Special Paper 97.

Zen, E. 1974. Prehnite- and pumpellyite-bearing mineral assemblages, west side of the Appalachian metamorphic belt, Pennsylvania to Newfoundland. Journal of Petrology, **15**: 197–242.

Zen, E. 1989. Tectonostratigraphic terranes in the northern Appalachians. Field Trip Guidebook T359, 28th International Geological Congress, Washington, D.C.